The influence of periodic wind turbine noise on infrasound array measurements

Article *in* Journal of Sound and Vibration · October 2016

DOI: 10.1016/j.jsv.2016.10.027

CITATIONS
12

READS
573

2 authors:

Christoph Pilger
Bundesanstalt für Geowissenschaften und Rohstoffe
91 PUBLICATIONS **263** CITATIONS
SEE PROFILE

L. Ceranna
Bundesanstalt für Geowissenschaften und Rohstoffe
141 PUBLICATIONS **1,238** CITATIONS
SEE PROFILE

Journal of Sound and Vibration 388 (2017) 188–200

Contents lists available at ScienceDirect

Journal of Sound and Vibration

journal homepage: www.elsevier.com/locate/jsvi

The influence of periodic wind turbine noise on infrasound array measurements

Christoph Pilger*, Lars Ceranna

Bundesanstalt für Geowissenschaften und Rohstoffe (BGR), Stilleweg 2, 30655 Hannover, Germany

ARTICLE INFO

Article history:
Received 1 March 2016
Received in revised form
14 September 2016
Accepted 13 October 2016
Handling Editor: Dr. A.V. Metrikine
Available online 28 October 2016

Keywords:
Infrasound
Wind turbine
Aerodynamic noise
Blade passing harmonics
CTBT

ABSTRACT

Aerodynamic noise emissions from the continuously growing number of wind turbines in Germany are creating increasing problems for infrasound recording systems. These systems are equipped with highly sensitive micro pressure sensors accurately measuring acoustic signals in a frequency range inaudible to the human ear. Ten years of data (2006–2015) from the infrasound array IGADE in Northern Germany are analysed to quantify the influence of wind turbine noise on infrasound recordings. Furthermore, a theoretical model is derived and validated by a field experiment with mobile micro-barometer stations. Fieldwork was carried out 2004 to measure the infrasonic pressure level of a single horizontal-axis wind turbine and to extrapolate the sound effect for a larger number of nearby wind turbines. The model estimates the generated sound pressure level of wind turbines and thus enables for specifying the minimum allowable distance between wind turbines and infrasound stations for undisturbed recording.

This aspect is particularly important to guarantee the monitoring performance of the German infrasound stations I26DE in the Bavarian Forest and I27DE in Antarctica. These stations are part of the International Monitoring System (IMS) verifying compliance with the Comprehensive Nuclear-Test-Ban Treaty (CTBT), and thus have to meet stringent specifications with respect to infrasonic background noise.

1. Introduction

Wind turbine noise [1] has an audible acoustic as well as an infrasonic component and it is important to keep this difference in mind when considering investigations both on human perception and instrumental detection capability. While the human perception is subject of previous studies (e.g. [2,3]) and ongoing discussions (e.g. [4,5,6] and references therein), this study solely focuses on the effects of the (impulsive) infrasonic component of wind turbine noise on infrasound measurements by microbarometer arrays.

Infrasound is sound at frequencies less than 20 Hz. It is generated by a large variety of natural and anthropogenic sources like meteoroids, volcanoes, earthquakes, severe weather, ocean waves, supersonic flights, quarry and mining activity and explosions [7]. Scientific studies on the infrasonic propagation [8,9], attenuation [10,11], detectability [12–14], source observations [15–18] and ambient noise [19,20] during the last years have successively improved the understanding of infrasound sources and processes. Apart from the mostly eruptive, explosive and convective sources mentioned above,

* Corresponding author.
E-mail addresses: christoph.pilger@bgr.de (C. Pilger), lars.ceranna@bgr.de (L. Ceranna).

http://dx.doi.org/10.1016/j.jsv.2016.10.027
0022-460X/

infrasound is also produced by large industrial activity, generators, moving machinery and wind turbines.

Comprehensive studies of acoustic emissions from various types of wind turbines already started in the seventies and eighties (e.g., references in [21]). The main focus of these investigations was in the audible frequency range above 20 Hz, since the low frequencies and intensities of infrasound from wind turbines cannot be heard or felt by people [22,23] and it was hardly possible to precisely measure wind turbine infrasound with standard microphones. Technological progress in this field and a revival of infrasound measurements as a verification technique for the Comprehensive Nuclear-Test-Ban Treaty (CTBT, www.ctbto.org) within the nineties also renewed and enhanced the interest for the infrasonic noise component of wind turbine sound emissions. More recent studies have been published on infrasound emission from wind turbines [24–26] and technical aspects of the wind turbine sound mechanisms [27–29].

Most of the sound emitted by modern wind turbines (three blades, horizontal axis, upwind orientation) is aerodynamic noise and has no prior-ranking mechanical reason like the sound of moving parts and electrical equipment [1,29]. Different aerodynamic mechanisms can be distinguished and include trailing edge and blade tip noise, inflow turbulence sound and impulsive signatures due to blade-tower interaction [21,29]. While the frequency range for the first processes mentioned is within the audible acoustics, the latter process has distinct frequency peaks located in the infrasonic frequency range. During each revolution, the blades are exposed to a load deficit caused by perturbed airflow upstream of the tower [24,28]. As the blades pass the tower, they encounter variations in the airflow generated by changes in wind direction and intensity when flowing around the wind turbine tower. This repetitive process generates impulsive sound signals consisting of a composition of pure tones which are integer multiples of the fundamental blade-passing harmonic (BPH) – the product of rotational speed and number of blades, e.g. see [24,30–32]. Moreover, the size of the blades and their low rotational speed of 10 to 30 revolutions per minute (rpm) yieldsound that is not primary situated in the audible frequency range, a large amount is emitted as infrasound below 20 Hz.

As the operator of currently three arrays of highly sensitive infrasound recording systems, the Bundesanstalt für Geowissenschaften und Rohstoffe (BGR, www.bgr-bund.de) is particularly interested in estimating the aerodynamic infrasonic noise signals generated by large wind turbines. Information on the frequency and intensity of these signals and their potential to interfere with CTBT monitoring and verification purposes in the most relevant frequency window between 0.02 and 4 Hz is essential for the I26DE infrasound station in the Bavarian Forest, and the I27DE infrasound station in Antarctica. These stations are part of the International Monitoring System (IMS) verifying compliance with the CTBT. Low infrasonic background noise at these stations is a pre-requisite for the detection of possible nuclear explosions in the atmosphere. Other IMS infrasound stations are already being disturbed by signals emitted by wind turbines. Near the I50UK station on Ascension Island, small wind turbines are increasing the noise level [32], and at I57US in southern California, a large wind farm at a distance of about 35 km occasionally causes short-term disturbances [26]. Wind turbine noise effects on seismometer stations have also been investigated and reported for example at AS104 station in Eskdalemuir, UK [27,34]. Stammler and Ceranna [35] investigate the increasing influence of wind turbines on seismic records, depending on the wind speed and on the number of newly build wind turbines in the vicinity of seismic sensors.

At the German infrasound stations I26DE and I27DE, the situation is different yet. Since 2005, there are frequent but unimplemented plans by the Bavarian state to set up wind turbines only a few kilometres from the I26DE infrasound array. With respect to the I27DE Antarctic station, there have been plans to build five 30 kW wind turbines to generate electricity for the nearby Neumayer III research base, of which only one has been erected so far. To avoid any degradation in the detection performance of I26DE and I27DE, it is necessary to determine the effect of wind turbines on the aerodynamic noise level at infrasound stations in relation to their distance.

To determine the emissions of infrasound signals by wind turbines, a field campaign was carried out north of Hanover near a single 200 kW horizontal-axis wind turbine. Furthermore, ten years of infrasound data at IGADE, the third German infrasound array, were analysed with respect to influences of nearby wind turbines. Section 2 describes the instruments and processing used within this study. Section 3 describes the observations and findings of wind turbine influences on infrasound records. Section 4 describes model calculations applied to theoretically quantify sound pressure levels (SPL) expected at wind turbinesound influenced stations and comparisons to the observed data. Further model calculations on the influence of single versus multiple wind turbines and the effect of ducting and propagation on the SPL of infrasound observations are also included in Section 4. Sections 5 and 6 present discussion and conclusions on minimum distances between infrasound arrays and wind turbines derived from the model calculations of SPLs in the infrasonic frequency range and verified by infrasound observations.

2. Instrumentation and data processing

2.1. Infrasound array IGADE

IGADE is a four element infrasound array in Northern Germany about 20 km to the north of Bremen. The station was installed between 2003 and 2005 and started continuous operations in 2005 until the present day. The station is similar in construction to the German IMS Station I27DE in Antarctica, and is frequently used as training station for Neumayer III staff (annual overwinter team) and for testing purposes and preparation of annual I27DE maintenance. The four elements are arranged in a triangle with about 800 m edge length, each element is equipped with a MB-2000 microbarometer, a digital

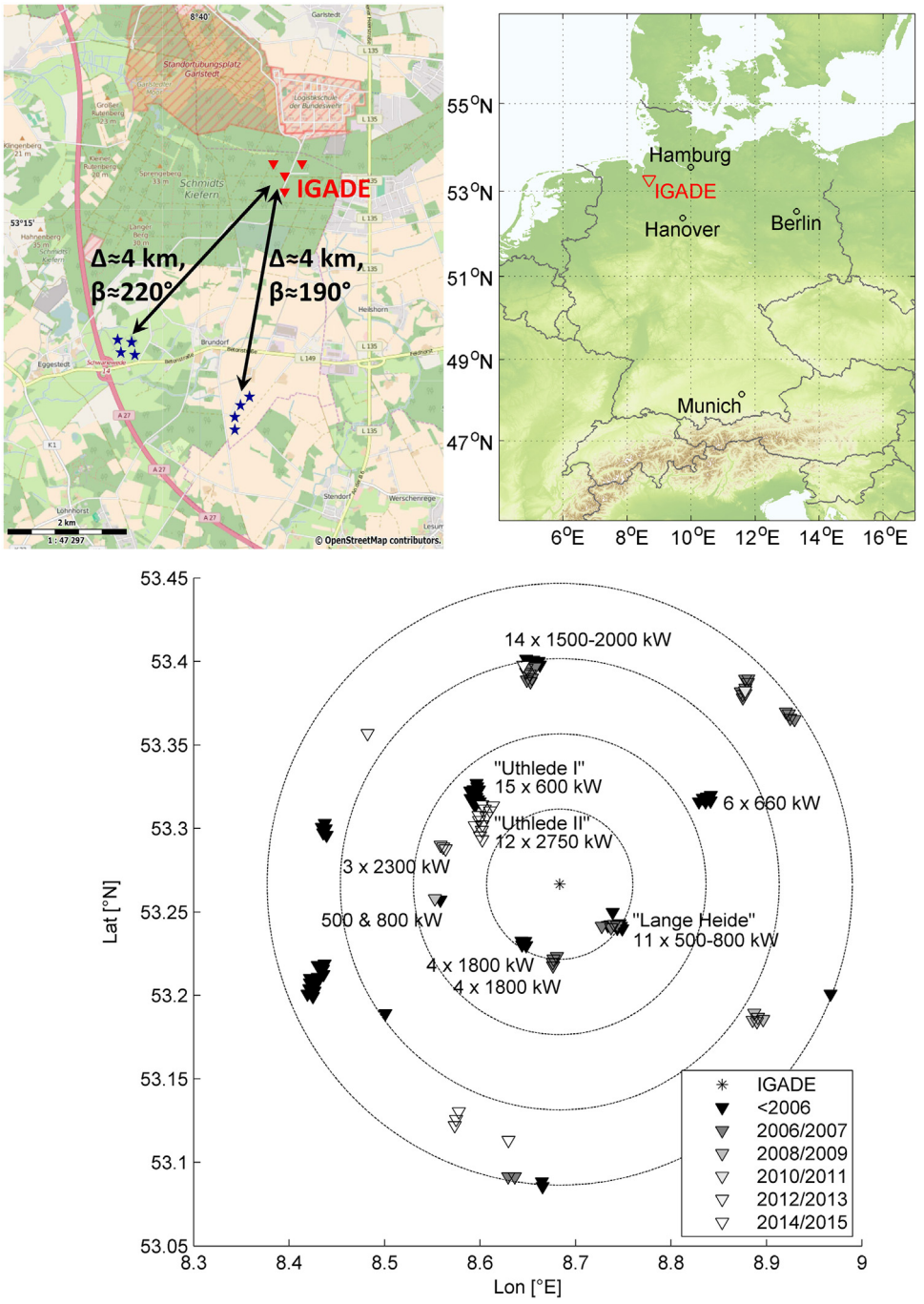

Fig. 1. Top left: Map with the configuration of the IGADE four element infrasound array (red triangles) and the position of nearby wind turbines (blue stars). Top right: Map of Germany including the position of IGADE (red triangle). Bottom: Past and current situation of wind turbines around IGADE. Black triangles show wind turbines continuously in operation during the 10 years of measurement duration (2006–2015), while grey to white triangles show wind turbines that were constructed during these years. Dashed circles show distances of 5, 10, 15 and 20 km to the station IGADE (star in the center). Rated power in kW is shown for turbines within 10 km distance. 118 wind turbines in total are situated in 20 km around IGADE. (For interpretation of the references to color in this figure legend, the reader is referred to the web version of this article.)

recording unit and a wind noise reduction system in the form of 15 m long star-shaped porous hoses (reader is referred to [36] for further information about micro pressure sensors and to [37] about wind noise reduction systems). IGADE is located in a dense forest nearby to a military area.

The closest wind turbines, four Enercon 1800 kW turbines close to each other with variable rotor speeds of 8 to 22.5 rpm, are located in south-western direction (220°) about four kilometers away. These turbines are in operation since 2005 or

earlier. Four more 1800 kW turbines are situated in about four kilometres distance in nearly southern direction (190°) and were constructed during 2006. Fig. 1 details the position and array geometry of IGADE as well as the location, distance and direction of nearby wind turbines. These two groups of wind turbines have the strongest impact on IGADE infrasound measurements as detailed in chapter 3. Other wind facilities in the vicinity of the station only have a secondary impact on infrasound measurements, which follows from their numbers, distances and power output as well as from the prevailing south-western wind direction at the IGADE site. These other wind facilities include the 4–5 km distant wind park Lange Heide (direction 120°) with 11 turbines of 500–800 kW constructed between 2001 and 2007 and the wind park Uthlede with 15 elements of 600 kW in about 8–9 km distance and 320° direction operational since 1998. The wind park Uthlede II with 12 elements of 2750 kW each in about 7–8 km distance (also 320° direction) started operations end of 2014 and might generate increasing wind turbine sound in the coming years. Further wind turbines are distributed with increasing distance in nearly all directions and sum up to a total number of 118 between four and 20 km, as shown in Fig. 1c. Their distance-dependent influence on infrasound measurements is especially related to their electric power output and numbers, which will be further investigated in chapter 4 of this study.

2.2. Field campaign with mobile infrasound sensors

In summer 2004, BGR carried out four weeks of fieldwork in Northern Germany using four mobile infrasound recording systems. The field campaign aimed at operating the mobile instruments near a single wind turbine providing a clear pressure signal, which allowed to define the correlation between source and recorded signals. It was difficult to fulfil the condition for a preferred minimum distance of approximately 5 km to other wind turbine given an average wind turbine density in Lower Saxony of about 1 per km^2 then [38]. Eventually, a single Vestas V47 200 kW wind turbine with fixed rotor speeds of 20 or 26 rpm was located close to Schwarmstedt, a small town about 20 km north of Hanover. The map in Fig. 2 shows the location of the wind turbine as well as the configuration of the field installations.

A total of eight measuring locations were selected along an approx. 2 km long west-east line to record the infrasound signals generated by the wind turbine. Each of the four mobile recording systems was equipped with a MB2000 micro-barometer and a 24-bit digitizer. The survey was divided into three consecutive periods to cover the eight measurement locations with the four mobile systems. From July 7th to 19th, the mobile systems were placed at sites 1 to 4; from July 19th to 29th at sites 1 and 5 to 7; and finally from July 29th to August 5th at site 8. At the latter location, all recording systems were installed in the form of a 4-element tripartite mini-array with an aperture of 35 m. This configuration was used to clearly identify signals from the wind turbine at a distance of 2 km because it was not clear whether these signals could be distinguished at this distance from the ambient background noise. It was hoped to identify the emitted signals by pointing the beam of the four array elements in the direction of the wind turbine because this technique is able to improve the signal-to-noise ratio by a factor of two. In order to obtain optimum recording conditions for infrasound signals at low ambient noise, the vegetation along the survey line at sites 1 to 7 was used to reduce wind effects. The small array around measuring point 8 was located in a small grove. Furthermore, spatial filters consisting of four 3 m long porous hoses were laid out on the ground. The sampling rate during the survey was 100 Hz.

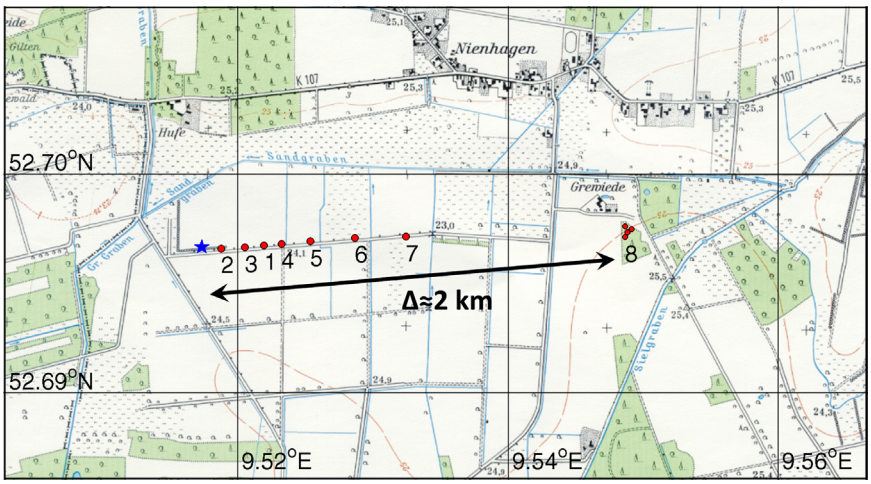

Fig. 2. Map showing the configuration of the 2004 field experiment for measuring infrasound generated by a single wind turbine about 20 km to the north of Hanover. The 8 sites are marked by red circles along a 2 km east-west line, the wind turbine is marked by a blue star. Mobile stations with an MB2000 micro pressure sensor each were installed at the sites 1 to 7. At site 8, a small four element triangular mini-array with a centre station and an aperture of 35 m was deployed. (For interpretation of the references to color in this figure legend, the reader is referred to the web version of this article.)

2.3. Infrasound data analysis (PMCC)

The Progressive Multi-Channel Correlation method (PMCC, [39]) is widely used as a real-time detector for multi channel infrasound raw pressure data to identify and analyse low-amplitude coherent waves within non-coherent noise, based on a progressive study of the correlation functions. The correlation functions are used to calculate the propagation time of a coherent wave between two sensors and thus to derive direction and velocity information from the occurring time shifts. PMCC was originally designed for seismic arrays, but also proved to be very efficient for infrasound array data.

Data from IMS and national infrasound stations are processed at the CTBTO and at National Data Centers as BGR using the PMCC method in order to generate automatic bulletins summarizing all detected coherent signals in infrasound frequency bands from high frequency signatures (HF, above 0.7 Hz) over so-called microbarom frequencies (MB, 0.7–0.05 Hz) down to long period mountain waves (MW, below 0.05 Hz). Parameters like onset time, duration, frequency, amplitude, apparent velocity (velocity of a wave-front observed between the infrasound array elements) and azimuth angle (direction from an observing station to the signal source, given in degrees clockwise from north) can be associated to a signal detection using PMCC, thus providing directional information about the signal origin.

3. Observations

3.1. Wind turbine noise and blade passing harmonics

The characteristics and influence of wind turbine noise on infrasound measurements were observed during more than ten years of operation of the four element infrasound array IGADE in Northern Germany (see Section 2.1).

Ten complete years of data between January 2006 and December 2015 were analysed in the course of this study with respect to the influence of wind turbine noise on infrasound recordings. Regular features at different distinct frequency values, the abovementioned BPH, were observed in sound pressure level calculations over the complete time duration (see Fig. 3a). At certain frequencies and during nearly all years and seasons, the aerodynamic sound waves of the BPH increases the SPL detected and quantified by the sensors. All SPL values presented within this study are based on root-mean-square (rms) values of the pressure fluctuation referenced to 20 μPa and are given in decibel (dB). The strongest BPH features observed in Fig. 3a can be identified around 1.3 – 1.4 Hz and multiples of this frequency (i.e. at ~2.7 Hz, ~4.1 Hz, ~5.4 Hz, ~6.9 Hz). 1.4 Hz is the second BPH for a rotor with an average speed of 14 rpm and BPHs with multiples of this frequency occur during most of the observations and with the highest spectral increase compared to neighbouring frequencies.

To associate these signatures to the source emissions of wind turbines, infrasound data analysis using the PMCC method (Section 2.3) can be applied. Daily PMCC bulletins were processed for the ten years, wherein nearly 620,000 high frequency infrasound ($f > 0.7$ Hz) source detections were identified. The azimuth directional information is extracted from these bulletins and shown in a histogram in Fig. 3b. The aerodynamic noise signals generated by the wind turbines can be clearly recognized in the figure as an accumulation of bearings with distinct peaks in station azimuth at approximately 190° and

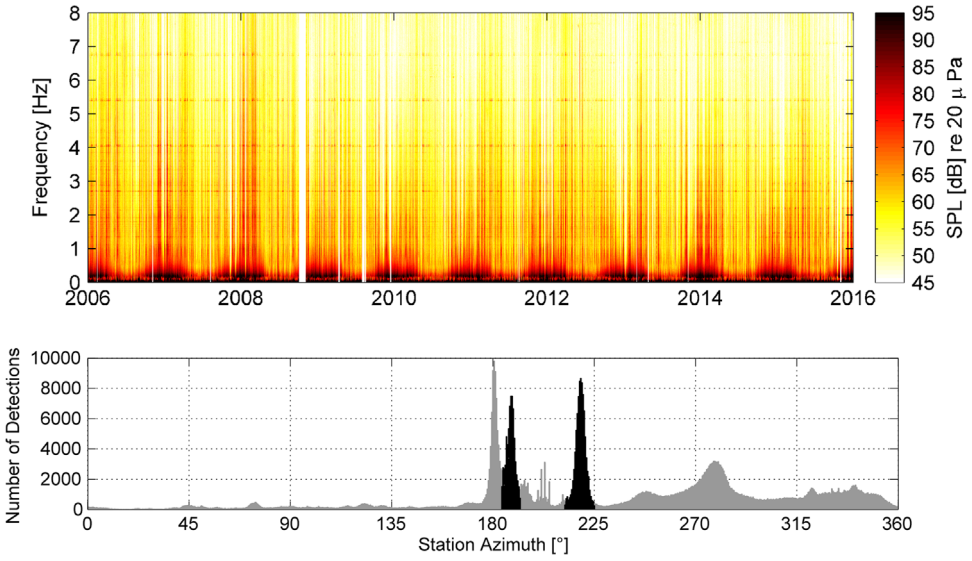

Fig. 3. Top: Calculation of sound pressure levels (SPL) for ten years of IGADE measurements (January 2006 to December 2015) for one element from 0 to 8 Hz. SPLs are color coded with horizontal lines of increased SPL clearly indicating wind turbine noise influences at certain frequencies. Bottom: Histogram showing the number of detections derived from PMCC at infrasound array IGADE in the 0.7 to 4.0 Hz frequency range as a function of station azimuth for the ten years period shown above. Detections related to the wind turbines are marked in black.

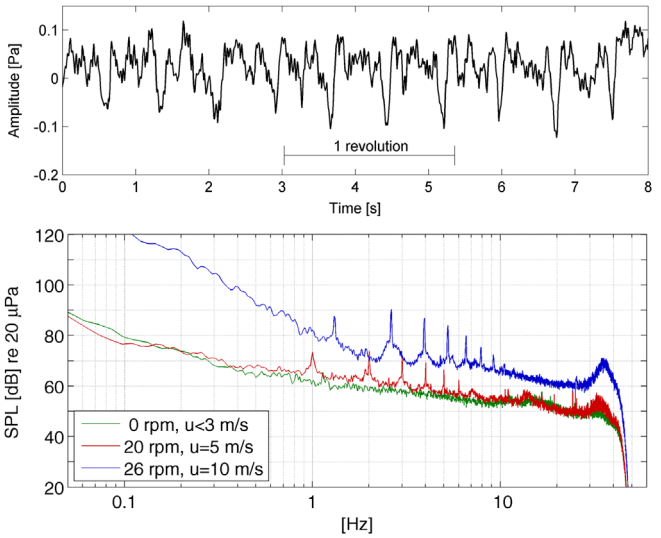

Fig. 4. Top: Eight seconds of sound pressure (7 July 2004, 23:54:22 – 23:54:30 UTC) recorded at field campaign site 3, filtered with a 0.5 Hz high-pass filter. Impulsive peak signatures that repeat with a 1–1.3 Hz frequency can be recognized in the time series. Bottom: Examples of the sound pressure level (SPL) recorded over 30 min at site 3 about 200 m away from the source. Each curve was measured at different prevailing wind speeds: no wind (green, 8 July 2004, 10:30–11:00 UTC), intermediate (red, 8 July 2004, 19:30–20:00 UTC), and high (blue, 10 July 2004, 12:40–13:10 UTC) wind speeds. The blade-passing harmonics appear as multiples of the fundamental harmonics at 1.0 Hz (20 rpm) and 1.3 Hz (26 rpm). (For interpretation of the references to color in this figure legend, the reader is referred to the web version of this article.)

220°, well in agreement with the direction towards nearby wind turbines (Fig. 1). These maxima of infrasound detections with one exception clearly exceed the level of detections of other, remote infrasound sources as for example supersonic military aircrafts registered from the North Sea (azimuths around 280°, see [10]) and other more sporadic sources. The highest peak in Fig. 3b is related to a steel-mill situated in southern (180°) direction and 20 km distance generating intense infrasound signatures with characteristics clearly different to those of wind turbines in their occurrence (during weekday working hours only) and independence of wind conditions. More than 25% of all detections with frequencies above 0.7 Hz come from the two (190° and 220°) wind turbine directions. Other wind parks in either larger distances or with lower power outputs seem to only have sporadic influences on the infrasound detections. While some signatures related to wind turbines are present in 120° and 320° directions, these numbers are quite sparse. It is expected that the number of wind turbine related detections towards 320° will strongly increase in the years after 2014, since a large number of high power output wind turbines started operations there lately. Because the number of wind turbine related noise detections at IGADE is high, the wind turbines significantly degrade the detection capability in large angular segments of about 10° azimuth towards each cluster of wind turbines as shown in Fig. 3b.

3.2. Correlation between aerodynamic noise and wind speed

Fig. 4a shows an eight second differential pressure time series recorded at one of the field campaign (Section 2.2) microbarometers during strong wind conditions. Intense, impulsive peak signatures with a repeating frequency of about 1.3 – 1.4 Hz can be observed in this short time series, well in agreement with the blade passing harmonics identified at IGADE in the previous section. The generated pressure signals show an impulsive characteristic, however, the pulses may change in amplitude and shape over time. The strong pulses are negative in this case, since the blade movement is directed away from the array. The upwind waveforms are the inverse (180° out of phase) of those measured downwind [21]. It seems evident that drag and lift change over time due to variable wind and airflow conditions and can therefore be different for each blade passing the tower. This refers to the fact that enhanced amplitude modulations during each revolution may result from turbulent airflow and/or wind shear at the tower superimposed on the mean wind field [33]. Thus, some blade-passages generate weaker or no pressure pulses. However, the blades passing the tower can be described as a sequence of pulsed acoustic signals with a fixed time delay Δt which is a function of the number of blades B and the rotational speed Ω, $\Delta t = (\Omega \cdot B)^{-1}$. In contrast to the time domain, these aerodynamic noise signals are represented by narrow band lines in the Fourier spectrum as a result of an ergodic process. These lines are observed at frequencies being whole-number multiples of the fundamental blade-passing harmonic (BPH), which is the reciprocal of Δt.

The sound pressure variations emitted by horizontal-axis wind turbines strongly depends on the rotational speed, which can be clearly observed in the field campaign case of the single Vestas V47 wind turbine designed for two distinct rotor speeds. The wind turbine operates in modes of 20 revolutions per minute (rpm) for weak and intermediate winds, and 26 rpm for stronger wind speeds exceeding 8 m/s, respectively. If the wind speeds at the hub are below 3 m/s, the blades stand still. Fig. 4b shows spectral curves for both rotational speeds as well as the curve for calm conditions for comparison.

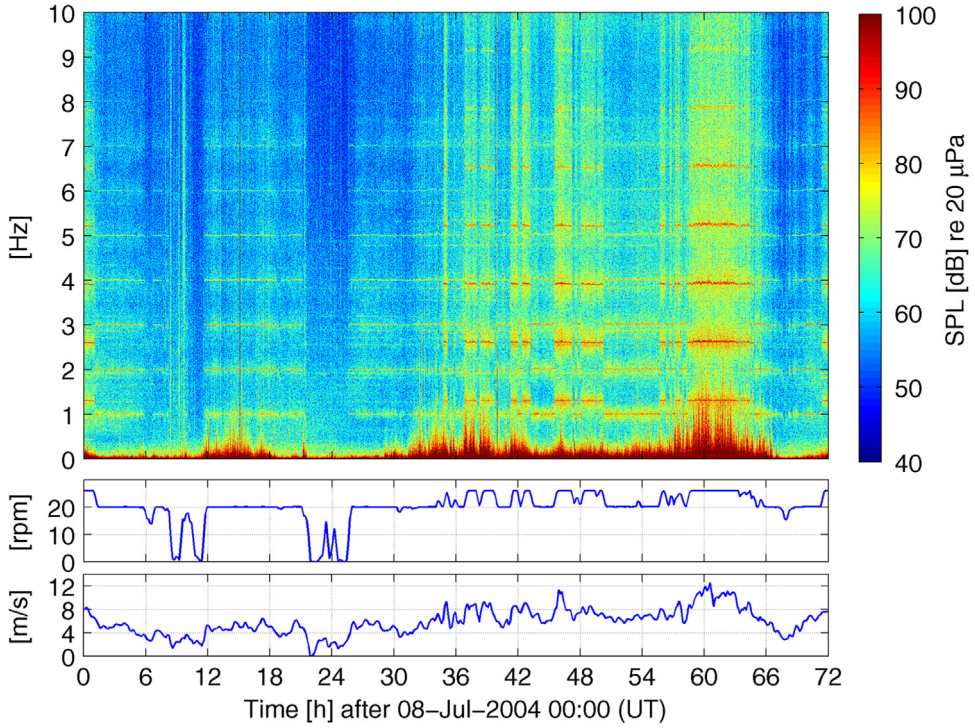

Fig. 5. Time-frequency analysis of pressure recordings at site 3 showing colour-coded sound pressure levels (SPL) over a period of 72 h, saturated at 100 dB. The lower two graphs show the corresponding rotational speeds of the wind turbine blades and the prevailing wind speeds at the hub.

Each spectrum is derived from 30 minutes of measurements at one microbarometer site selected during continuous wind conditions and corresponding rotational speeds of the wind turbine of 26, 20 and zero rpm. The increase in the background noise with increasing wind speeds is clearly visible, as well as the spectral peaks of the blade-passing harmonics as multiples of $(\Delta t)^{-1} = ((20\ or\ 26)/60s)\cdot 3 = 1.0\ or\ 1.3\ Hz$. A widening in the basis of the spectral peaks for the first harmonics is obvious. This widening is caused by proximal measurements, i.e. at distances to the source of less than three to five wavelengths. The harmonics are not fully established in the proximal field, which means that the vibrations of the blades and the tower (usually weaker than the harmonics) may also contribute to the low frequency noise of the wind turbine.

The time-frequency analysis in Fig. 5 further demonstrates the correlation between the emitted SPL and the rotational as well as the wind speeds. For a period of 72 h, the average SPL at consecutive five minutes intervals is calculated and plotted against the rotational speed of the wind turbine, as well as the wind speed measured at the hub. The strong impact of the aerodynamic noise generated by wind turbines on infrasound recording systems becomes clearly visible, in particular at the time interval from 36 to 66 h. At field campaign site 3, about 200 m from the wind turbine, the signal immissions exceed the background noise at frequencies below 10 Hz by up to 20 dB, and approximately 10 dB at high and intermediate wind speeds. Overall, the field measurements showed the strength of infrasound emissions by wind turbines. At frequencies above 10 Hz in particular, no harmonics were measured by the MB2000 micro-barometers. This is not caused by the instruments, since they have an upper 3-dB point at 27 Hz defining the high-frequency limit of sensitivity, but rather by the spatial filters used for the recordings at ground level and by the masking of higher harmonics by the background and wind noise which exceeds the lower level amplitudes of higher harmonics.

4. Modelling

4.1. Estimating the sound pressure level of the harmonics

Many papers [21,26,33,34,40] have been written on impulsive peaks in the sound pressure level generated by the passing blades of wind turbines. Viterna [30] provides a concise and convenient method of calculating the SPL of the BPH as a function of wind turbine design parameters. His approach is based on studies published by Sears [41] and Lowson [42] and takes discontinuous aerodynamic blade forces into account. The time dependent forces on the blades are represented by complex Fourier coefficients corrected by the Sears function to account for the aerodynamic effects on blades when passing the tower and encountering abrupt changes in lift and drag. Viterna [30] derived the following expression for the average free field sound pressure p_n of the n^{th} blade-passing harmonic generated by horizontal-axis wind turbines:

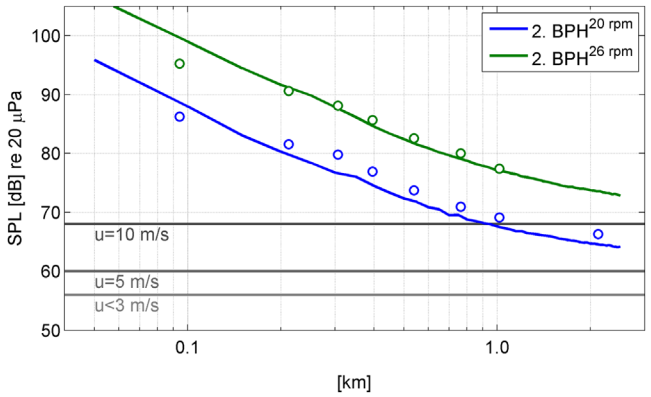

Fig. 6. Comparison of the computed (-) and the measured (o) sound pressure level (SPL) of the second blade-passing harmonic (BPH) considering rotational speeds of 20 and 26 rpm, blue and green respectively. The horizontal lines mark the average background noise level measured at less than 3 m/s, 5 and 10 m/s. (For interpretation of the references to color in this figure legend, the reader is referred to the web version of this article.)

$$p_n(d) = \frac{k_n\sqrt{2}}{4\pi d}\sum_m (e^{im(\theta-\pi/2)}J_x(k_nR_e\ \sin\ \gamma))\cdot\left(a_m^T\ \cos\ \gamma - \frac{nB-m}{k_nR_e}a_m^Q\right), \tag{1}$$

where m is the index of the blade harmonics ($m=\ldots-2,-1,0,1,2,\ldots$), $k_n=nB\Omega/c_0$ is the wave-number, B is the number of blades, Ω is the rotational speed, and c_0 is the sound speed. J_x is the Bessel function of first kind and xth order, where $x=nB-m$. R_e is the effective blade radius (75% of the blade radius), d the distance from the hub to the listener, γ and θ are the azimuth and the incidence angle to the listener, respectively. Finally, a_m^T and a_m^Q are the complex Fourier coefficients of thrust and torque derived from [30,41] to determine the unsteady flow associated with periodic variations of the wind velocity.A wind velocity deficit of 20% in a 30° angular segment between tower and blades is used in [30] for a downwind-oriented turbine, a deficit in the same order of magnitude is assumed within this study to simulate flow instabilities and blade-tower interaction also for modern, upwind-oriented turbines.

4.2. Comparing calculated and measured data

A comparison between the field campaign measurements and theoretical SPL using Eq. (1) is made in Fig. 6 for the whole range of 2 km considering rotational speeds of 20 and 26 rpm. Because only moderate wind speeds prevailed during the measurements at site 8 from July 29th to August 5th, 2004, there is no aerodynamic noise value at 2 km from a fast rotating turbine. The measured values are derived by averaging the sound pressure level during all time periods with prevailing easterly or westerly winds and the wind turbine rotating with either 20 rpm or 26 rpm. The total measurement duration for the 20 rpm case were 117 hours for sites 1–4, 107 hours for sites 5–7 and 101 hours for site 8, while for the 26 rpm case it were 63 hours for sites 1–4 and 3 hours for sites 5–7. The 2nd BPH (at its maximum level) is considered because it has the strongest spectral amplitude and therefore has the best chance of being observed at all sites. This can be taken from the calculated values at 2 km distance in Fig. 6 which are only 5 dB above the corresponding average background noise, shown by horizontal lines in the lower part of the figure. In general, good agreement between measured and theoretical values is observed, except at location 1 at a distance of only 100 m. This difference is due to the fact that the signals were recorded in the proximal field at distances of a single wavelength. However, the theoretical model in Eq. (1) describes the SPL in the distal field of a wind turbine, and may therefore overestimate the measured values of the BPHs in the infrasonic frequency range in the near field.

Because only the pure SPL of the harmonics can be calculated from Eq. (1), the underlying background noise was added using an average of the four instruments in a frequency window of 1.5–3.5 Hz derived during the occurrence of corresponding wind speeds of 10, 5 and <3 m/s. Furthermore, the local meteorological conditions during the measurements have to be accounted for in addition to the topography within the investigation area [30]. Both conditions have an impact on sound propagation and may on average increase the SPL by 3 to 6 dB. This is due to a combination of two effects, on the one hand focussing of sound not only propagating directly from wind turbine to receiver but also via reflections by the ground and the near-surface atmospheric boundary layer, on the other hand scattering of sound by rough topography at the surface and turbulence within the atmospheric boundary layer (see [26,43]). These effects are considered within this study by applying a 3–6 dB increase to the SPL. Taking this correction into account the measured values agree very well with the model calculations of SPL related to wind turbine sound emissions, as shown in Fig. 6.

Table 1
List showing the evolution of design parameters for horizontal-axis wind turbines over the last 25 years (source: Bundesverband WindEnergie e.V.).

Year	Hub height [m]	Blade diameter [m]	Total height [m]	Rated Power [kW]
1990	31	23	42	172
1995	47	39	66	480
2000	70	58	99	1115
2005	89	73	125	1710
2010	99	80	139	1994
2014	115	93	159	2593

4.3. *Different wind turbine parameters and wind farms*

Fig. 6 indicates that the detection of aerodynamic noise by a wind turbine at infrasound sensors is possible at distances up to 2 km, particularly because the signal-to-noise ratio was improved by a factor 2 (6 dB) by the beam-forming process applied to the records of the 4-element mini-array in 2 km distance. Therefore, it is justifiable to conclude that the emitted noise up to this distance lies at least in the range of the background noise level, if not above. However, this applies only to the particular single 200 kW wind turbine investigated during the 2004 field campaign and not to larger turbines with higher power output or even wind farms with a larger number of collocated turbines. It is important to note that during the last decades there has been an increasing trend to build higher wind turbines with larger rotors. These generate more electric power because the greater height above the ground ensures more constant wind conditions. Modern wind turbines now have hub heights of 100 m and more, with associated increases in the rotor diameter and blade tip speed. This increase also leads to higher sound pressure output and larger propagation distance of instrumentally detectable aerodynamic noise. In the following, different wind turbines are studied with respect to their potential infrasound emissions. Their design parameters are listed in Table 1, average values used for SPL modelling are listed in Table 2.

Fig. 7 based on Eq. (1) shows the computed characteristics of the SPL as a function of distance for the 2nd BPH considering the parameters listed in Tables 1 and 2. In essence, a strong increase in the aerodynamic SPL can be observed between the 200 kW turbine and next generation wind turbines with 1 MW power output and more. A large difference is therefore apparent in the distance before the background noise level is reached, this distance changes from a few kilometres for the 200 kW turbine to about 10–15 km for modern wind turbines. At such large distances, the aerodynamic noise of wind turbines is still instrumentally detectable when the SPL exceeds the background noise level at a recording infrasound station.

This background noise level represents the activity of different sources of ambient noise of either natural or anthropogenic origin. Wind contributes most to the background noise level, especially in the surface-near boundary layer. Wind eddies due to convection and wind shear are the dominant noise source at frequencies around 1–2 Hz. The noise level indicated by a horizontal bar in Fig. 7 (and 8) is 50($\pm$4) dB, which is the average level for background noise between 1 and 2 Hz at the IMS station I26DE. This station was chosen to represent background values at a site currently unaffected by wind turbine noise. Bowman et al. [19] compared the noise levels of 21 infrasound stations around the world, of which 16, like I26DE, are part of the IMS. They found that the average background noise level in the 1 to 2 Hz range is 54 dB, corresponding to the upper bound of the grey bar in Fig. 7. The variation of this value due to stations at different locations and surrounding conditions worldwide and due to diurnal and seasonal changes is in the order of 30 dB (at 1 Hz), thus resulting in individual station background noise levels of about 40–70 dB.

Fig. 8 reveals the effect of a wind farm of four or 16 elements with 1800 kW each, in contrast to a single turbine of the same category. There is a direct dependence between the increase in the number of turbines and the SPL of aerodynamic noise: the SPL of an N-element wind farm can be estimated by adding $20 \cdot \log_{10}(\sqrt{N})$ [dB] to the curve of a single wind turbine. The sound pressure grows proportional to the square root of the number of turbines, analogous to the relation for improving the signal-to-noise ratio in array theory [44]. In the case of a 16-element wind farm with 1800 kW wind turbines, the emitted aerodynamic noise is still above the background noise level at a distance of approximately 50 km. However, this

Table 2
Design parameters used for the modeling of SPL. Types 1–6 are sorted by rated power and use the same hub height, blade diameter and total height values as in Table 1.

Type	Rated Power [kW]	Number of Blades	Rotor Speed [rpm]	2. BPH [Hz]
1	200	3	26	2.6
2	500	3	22	2.2
3	1200	3	18	1.8
4	1800	3	14	1.4
5	2000	3	12	1.2
6	2600	3	10	1.0

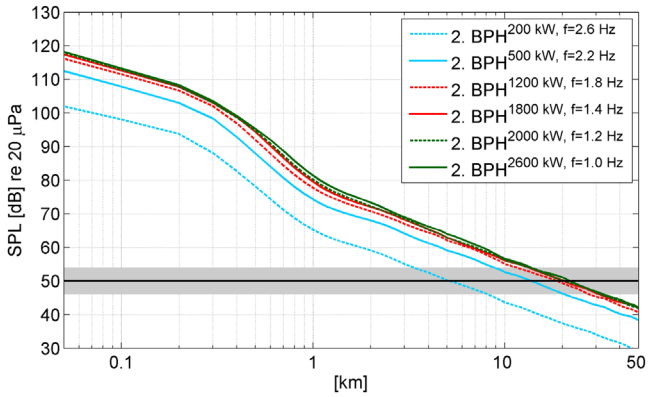

Fig. 7. Computed sound pressure level (SPL) of the second blade-passing harmonic (BPH) as a function of distance and the wind turbine design parameters summarized by the power output. The horizontal black line marks the average background noise level between 1 and 3 Hz at I26DE, the grey bar shows its variation.

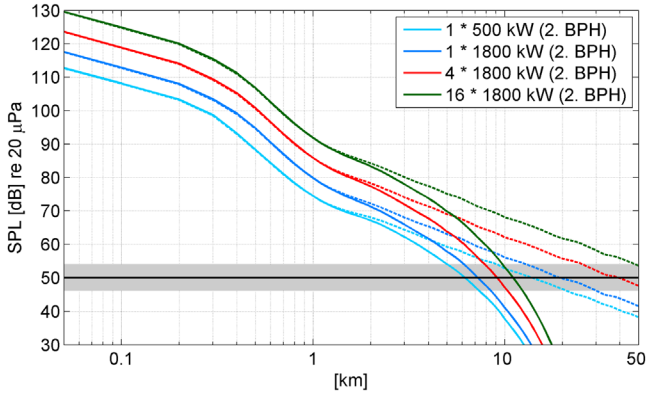

Fig. 8. Same as Fig. 7, but for different power output and numbers of wind turbines, also considering the existence of a tropospheric duct (dashed lines) and its absence (solid lines).

estimate is based on wind turbines running in phase and providing constructive interference [40]. Usually, this assumption is incorrect because each turbine runs at a different phase to deliberately avoid constructive interference which may damage the turbines. Nevertheless, this measure only has a minor effect on reducing aerodynamic noise in the distal field. Studying seismic recordings of quarry blasts, Mc Laughlin et al. [45] showed that the constructive interference of surface waves in the distal field remains almost unaffected by time delays in the detonation of explosive charges. In this analogy, the time delays of the detonations correspond to different phase angles of the wind turbines. Furthermore, the propagation of seismic surface waves is equivalent to sound propagation ducted close to the surface. Therefore, wind farms can also produce constructive interference in the distal field with the emitted acoustic energy being independent of phase angles.

4.4. Wind effects on geometrical spreading

The decrease of pressure with distance in Eq. (1) is governed by geometrical spreading of $1/d$ (spherical spreading), which is not necessarily justified for distances above 2 km. Numerical simulations of synthetic amplitude decay using the parabolic equation method [46] have been calculated for situations with and without a tropospheric duct (compare results shown in [47]) and revealed the following: in the case of a tropospheric duct with ideal wind and temperature conditions, sound pressure falls with values from $\sqrt{(1/d)}$ (cylindrical spreading) to $1/d$ up to distances of 50 km. Tropospheric ducts occur, when the effective sound speed (temperature-dependent phase velocity plus wind speed) in a layer of a few hundred meters to a few kilometres altitude is higher than the sound speed at the ground [47,48]. This leads to infrasound propagation with almost no additional attenuation, comparable to the propagation of light in optic fibres. However, tropospheric ducts are rare, less than 5% of the infrasonic energy is in general ducted in the troposphere outside regions associated with strong tropospheric jet streams, where the fraction is up to 20% [8]. Furthermore tropospheric ducts can be destabilized and dissolved after short distances due to surface-near instabilities in the temperature and wind conditions. Therefore, the absence of tropospheric ducts is more probable and for such atmospheric conditions the simulations reveal a

linear increase beyond 1/d geometrical spreading loss. It starts with 1/d and reaches $1/d^{2.5}$ at about 20 km distance, which is then a stable relation for the sound pressure amplitude versus distance decrease. These synthetic results are in accordance with observations made by Mutschlecner et al. [49], analyzing tropospheric infrasound signals from explosions. They found that the attenuation with distance for pressure amplitude of infrasound in the troposphere is very uniform and relative to $1/d^{2.5}$ for distances ranging from 17 to 269 km. Taking this and the considerations made in the previous paragraphs into account, the sound pressure level of the aerodynamic noise generated by a single wind turbine or a multi-element wind farm can be estimated as follows:

$$SPL_n(d) = 20\cdot\log_{10}\left(\frac{p_n(d)}{2\cdot10^{-5}}\right) + X_S + 20\cdot\log_{10}\left(\sqrt{N}\right) - 20\cdot\log_{10}\left(d^{\lambda}\right), \tag{2}$$

where p_n is the distance-dependent sound pressure of the nth blade-passing harmonic (see Eq. (1)), X_S is the site effect ranging from 3 to 6 dB due to topography and local meteorological conditions, N is the number of wind turbines, and d is the distance between sensor and wind turbine or wind farm. λ is the value for the spreading correction: either 0 in the case of an existing tropospheric duct, or a value increasing linear from 0 to 1.5 in 0 to 20 km and having a stable value of 1.5 above 20 km, if no duct is present. This spreading correction sums up together with the first term to a pressure amplitude attenuation relative to $1/d^{2.5}$ above 20 km.

Fig. 8 shows the results obtained by applying Eq. (2) to one, four and 16 wind turbines. The area affected by aerodynamic noise depends on the presence (dashed lines) or absence (solid lines) of tropospheric ducts. For a single modern (high kW output) wind turbine, the minimum distance to an IMS infrasound station being undisturbed from infrasonic aerodynamic noise is about 20 km considering ideal propagation in a tropospheric duct and is below 10 km assuming only occasionally stable tropospheric ducts. For a 16-element (1800 kW each) wind farm, the minimum distance for undisturbed recordings of an IMS infrasound station like I26DE is above 50 km with ideal propagation in a tropospheric duct and between 10 and 15 km when assuming only occasionally stable tropospheric ducts.

5. Discussion

The theoretically estimated minimum distances of 20 to 50 km between a single wind turbine or 16-element wind farm and an infrasound array seems to be rather large. However, recordings at the I57US IMS infrasound station at Piñon Flat in southern California have proven that coherent aerodynamic noise signals from a wind farm 35 km away can be detected (compare [26]). Although the wind farm is the third largest in California, and the signals are only sporadically detected, the result underscores that the estimated distances are realistic with respect to the tropospheric conditions. When considering that tropospheric ducting from wind turbines to infrasound arrays only sporadically occurs, the minimum distance for undisturbed detection performance most of the time reduces to 5 to 10 km for a single wind turbine and 10 to 15 km for a larger wind farm.

In general, the detection capability of an infrasound array with respect to transient signals is only reduced by noise disturbances if their intensity is similar or higher than the signal to be detected and their bearings, apparent velocities and frequency content are identical or very close to each other. If these values are different, the detection capability is only slightly degraded. Precisely this effect was observed during the 2004 field campaign when infrasound signals from a gas pipeline explosion near the Belgian capital Brussels were recorded by the mini-array at site 8 on 30 July 2004 [50]. The explosion was clearly detected because the signal parameters were completely distinct from the noise coming from the wind turbine. It should thereby be possible to apply narrowband filters for wind turbine noise from known directions and with known signal characterictics. Nevertheless, due to the large variability of the atmosphere as a propagation medium for infrasonic signals, these characteristics may change in such manner that wind turbine signatures filters might fail from case to case and an undisturbed measurement performance of stations in the vicinity of wind turbines is rendered impossible.

Influences of vegetation on the attenuation of wind turbine infrasound and thus reduction of minimum distance of undisturbed performance are only of second order and not incorporated in the calculations above. Vegetation can mostly be ignored with respect to infrasound attenuation due to the fact that the considered infrasonic wavelengths of the wind turbine noise of about 50 to 500 m are much larger than the typical sizes of trees. Nevertheless, vegetation reduces the background noise level at an infrasound station by a general reduction of small-scale turbulence, wind shear and eddies within wind-sheltered forest areas, thus allowing lower signal levels of infrasound from wind turbines to still be detected. The chosen background noise level of 50 dB related to IMS station I26DE takes this into account, since this station is located in the dense Bavarian forest, where vegetation reduces the ambient noise levels.

The effects of a wind farm on the detection capability of a nearby infrasound array became apparent at station IGADE north of Bremen. The array is only 4–5 km away from two small wind farms of currently four 1800 kW elements each (compare middle curve in Fig. 8) and various other wind parks witheven more elements in higher distances. During the planning phase of the infrasound station in 2004, there was only one wind turbine installed; the number has strongly increased shortly after that time and the effects of wind turbine noise are clearly observable in the sound pressure levels at the IGADE array elements. Due to the small distance, the wind turbine effects are present in the recordings independent of tropospheric ducting conditions most of the time. More than 25% of all high frequency infrasound detections at IGADE can

be associated to aerodynamic noise of nearby wind turbines degrading the detection capability of the array in these directions, which again clearly underscores the effect of wind turbine noise on infrasound observations and measurement performances.

Overall, these results highlight that it is essential to define minimum distances between infrasound stations and wind turbines which take into account their design parameters and number, especially for IMS stations, to guarantee their monitoring performance in the context of the CTBT and reduce the influence of wind turbine noise on these stations to a minimum.

6. Conclusions

This study provides all the necessary procedures for estimating the minimum allowable distance between wind turbines and infrasound stations to guarantee undisturbed recordings. Essential data was provided by the field campaign measurements at a single wind turbine north of Hanover and during ten years of operation of the infrasound array IGADE north of Bremen. Model estimations of the sound pressure level of aerodynamic noise generated by wind turbines as a function of their design parameters, number and distance to a receiver were performed within this study. Verification of these model estimations were performed by comparison of the model-derived BPHs within the infrasound frequency range with measurements of BPH signatures at different distances, rotor speeds and wind conditions during the field campaign at a 200 kW wind turbine. Minimum distances of detectability depending on the power output and number of wind turbines as well as influences of tropospheric ducting conditions were identified, modeled and quantified as core result of this study.

As a rule, a distance of 20 km should be kept between an infrasound station and a single wind turbine to guarantee unhindered recording and detection conditions. The distance would need to increase to 50 km in the case of a multi-element wind farm. However, when considering geometrical spreading and only occasional tropospheric ducts, a distance of 5 to 10 km to a single wind turbine and 10 to 15 km to a wind farm also appears to be adequate and sufficient to allow unhindered recording and detection conditions for an infrasound array especially in the context of preserving its nuclear monitoring capabilities.

Acknowledgements

We thank the shareholders of the “citizen-owned wind turbine Schwarmstedt” for providing us comprehensive, time-dependent data of the single wind turbine rotational velocity and corresponding wind-speed measurements at the turbine hub.

We are grateful to Gernot Hartmann, Nicolai Gestermann, Erwin Hinz and Torsten Grasse for their support in installing and maintaining the mobile infrasound stations during the field campaign.

References

[1] R. Bowdler, G. Leventhall (Eds.), *Wind Turbine Noise*, Multi-Science Publishing Co Ltd. ISBN: 978-1907132308, 2011.
[2] L.S. Whittle, S.J. Collins, W. Robinson, The audibility of low-frequency sounds, *J. Sound Vibr.* 21 (1972) 431–448, http://dx.doi.org/10.1016/0022-460X(72)90828-0.
[3] H. Møller, J. Andresen, Loudness of pure tones at low and infrasonic frequencies, *J. Low Freq. Noise Vibr.* 3 (1984) 78–87.
[4] E. Pedersen, F. van den Berg, R. Bakker, J. Bouma, Response to noise from modern wind farms in The Netherlands, *J. Acoust. Soc. Am.* 126 (2) (2009) 634–643, http://dx.doi.org/10.1121/1.3160293.
[5] R.J. Mc Cunney, K.A. Mundt, W.D. Colby, R. Dobie, K. Kaliski, M. Blais, Wind turbines and health: a critical review of the scientific literature, *J. Occup. Environ. Med.* 56 (11) (2014) 108–130, http://dx.doi.org/10.1097/JOM.0000000000000313.
[6] R.G. Berger, P. Ashtiani, C.A. Ollson, M. Whitfield Aslund, L.C. McCallum, G. Leventhall, L.D. Knopper, Health-based audible noise guidelines account for infrasound and low-frequency noise produced by wind turbines, *Front. Public Health* 3 (31) (2015) 1–14, http://dx.doi.org/10.3389/fpubh.2015.00031.
[7] P. Campus, D.R. Christie, Worldwide observations of infrasonic waves, in: A. Le Pichon, E. Blanc, A. Hauchecorne (Eds.), *Infrasound Monitoring for Atmospheric Studies*, Springer, Heidelberg. ISBN: 978-1-4020-9507-8, 2010.
[8] D.P. Drob, J.M. Picone, M.A. Garcés, Global morphology of infrasound propagation, *J. Geophys. Res.* 108 (2003) 4680, http://dx.doi.org/10.1029/2002JD003307.
[9] D.P. Drob, M. Garcés, M.A.H. Hedlin, N. Brachet, The temporal morphology of infrasound propagation, *Pure Appl. Geophys.* 167 (2010) 437–453, http://dx.doi.org/10.1007/s00024-010-0080-6.
[10] L.C. Sutherland, H.E. Bass, Atmospheric absorption in the atmosphere up to 160 km, *J. Acoustic Soc. Am.* 115 (2004) 1012–1032, http://dx.doi.org/10.1121/1.1631937.
[11] A. Le Pichon, L. Ceranna, J. Vergoz, Incorporating numerical modeling into estimates of the detection capability of the IMS infrasound network, *J. Geophys. Res.* 117 (2012) D05121, http://dx.doi.org/10.1029/2011JD016670.
[12] A. Le Pichon, J. Vergoz, P. Herry, L. Ceranna, Analyzing the detection capability of infrasound arrays in Central Europe, *J. Geophys. Res.* 113 (2008) D12115, http://dx.doi.org/10.1029/2007JD009509.
[13] D.N. Green, D. Bowers, Estimating the detection capability of the International Monitoring System infrasound network, *J. Geophys. Res.* 115 (2010) D18116, http://dx.doi.org/10.1029/2010JD014017.
[14] C. Pilger, L. Ceranna, J.O. Ross, A. Le Pichon, P. Mialle, M.A. Garcés, CTBT infrasound network performance to detect the 2013 Russian fireball event, *Geophys. Res. Lett.* http://dx.doi.org/10.1002/2015GL063482.
[15] L. Evers, H.W. Haak, The detectability of infrasound in The Netherlands from the Italian volcano Mt. Etna, *J. Atmos. Solar-Terrestrial Phys.* 67 (2005) 259–268, http://dx.doi.org/10.1016/j.jastp.2004.09.00.

[16] L. Ceranna, A. Le Pichon, D.N. Green, P. Mialle, The Buncefield explosion: a benchmark for infrasound analysis across Central Europe, *Geophys. J. Int.* 177 (2009) 491–508, http://dx.doi.org/10.1111/j.1365-246X.2008.03998.x.
[17] D.N. Green, R.S. Matoza, J. Vergoz, A. Le Pichon, Infrasonic propagation from the 2010 Eyjafjallajökull eruption: investigating the influence of stratospheric solar tides, *J. Geophys. Res.* 117 (2012) D21202, http://dx.doi.org/10.1029/2012JD017988.
[18] A. Le Pichon, L. Ceranna, C. Pilger, P. Mialle, D. Brown, P. Herry, N. Brachet, The 2013 Russian fireball largest ever detected by CTBTO infrasound sensors, *Geophys. Res. Lett.* 40 (2013) 3732–3737, http://dx.doi.org/10.1002/grl.50619.
[19] J.R. Bowman, G.E. Baker, M. Bahavar, Ambient infrasound noise, *J. Geophys. Res.* 32 (2005) L09803, http://dx.doi.org/10.1029/2005GL022486.
[20] R.S. Matoza, M. Landès, A. Le Pichon, L. Ceranna, D. Brown, Coherent ambient infrasound recorded by the International Monitoring System, *Geophys. Res. Lett.* 40 (2013) 429–433, http://dx.doi.org/10.1029/2012GL054329.
[21] H.H. Hubbard, K.P. Shepherd, Aeroacoustics of large wind turbines, *J. Acoust. Soc. Am.* 89 (1991) 2495–2508, http://dx.doi.org/10.1121/1.401021.
[22] G. Leventhall, Infrasound from wind turbines – fact, fiction or deception, *Can. Acoust.* 34 (2) (2006) 29–36.
[23] G. Leventhall, Concerns about infrasound from wind turbines, *Acoust. Today* 9 (3) (2013) 30, http://dx.doi.org/10.1121/1.4821143.
[24] J. Jakobsen, Infrasound emission from wind turbines, *J. Low Freq. Noise, Vibr. Active Control* 24 (3) (2005) 145–155.
[25] S.S. Jung, W. Cheung, C. Cheong, S. Shin, Experimental identification of acoustic emission characteristics of large wind turbines with emphasis on infrasound and low-frequency nnoise, *J. Korean Phys. Soc.* 53 (4) (2008) 1897–1905, http://dx.doi.org/10.3938/jkps.53.1897.
[26] O. Marcillo, S. Arrowsmith, P. Blom, K. Jones, On infrasound generated by wind farms and its propagation in low-altitude tropospheric waveguides, *J. Geophys. Res.* 120 (2015) 9855–9868, http://dx.doi.org/10.1002/2014JD022821.
[27] Styles, P., R. F. Westwood, S. M. Toon, M.-P. Buckingham, B. Marmo, B. Carruthers, Monitoring and Mitigation of Low Frequency Noise from Wind Turbines to Protect Comprehensive Test Ban Seismic Monitoring Stations, Proceedings of the Fourth International Meeting on Wind Turbine Noise (2011), 13p.
[28] C.J. Doolan, D.J. Moreau, L.A. Brooks, Wind turbine noise mechanisms and some concepts for its control, *Acoust. Australia* 40 (1) (2012) 7–13.
[29] R. Tonin, Sources of wind turbine noise and sound propagation, *Acoustics Australia* 40 (1) (2012) 20–27.
[30] Viterna, L. A., The NASA-LERC wind turbine noise prediction code, DOE/NASA/20366-1, NASA TM-81737 (1981).
[31] G.P. Van den Berg, The beat is getting stronger: the effect of atmospheric stability on low frequency modulated sound of wind turbines, *J. Low Freq. Noise, Vibr. Active Control* 24 (2005) 1, http://dx.doi.org/10.1260/0263092054037702.
[32] CTBTO Spectrum, Installing IS50 on Ascension Island: green turtles and mysterious data spikes, CTBTO Newsletter 9 (January 2007), 12-15.
[33] Oerlemans, S., An explanation for enhanced amplitude modulation of wind turbine noise, NLR-Report, NLR-CR-2011–2071 (2011).
[34] Styles, P., R. England, I. G. Stimpson, S. Toon, D. Bowers, M. Hayes, A Detailed Study of the Propagation and Modelling of the Effects of Low Frequency Seismic Vibration and Infrasound from Wind Turbines, Proceedings of the First International Meeting on Wind Turbine Noise (2005), 27p.
[35] K. Stammler, L. Ceranna, Influence of wind turbines on seismic records of the Gräfenberg array, *Seismol. Res. Lett.* 87 (5) (2016) 1–10, http://dx.doi.org/10.1785/0220160049.
[36] D. Ponceau, L. Bosca, Low-noise broadband microbarometers, in: A. Le Pichon, E. Blanc, A. Hauchecorne (Eds.), *Infrasound Monitoring for Atmospheric Studies*, Springer, Heidelberg. ISBN: 978-1-4020-9507-8, 2010.
[37] K.T. Walker, M.A.H. Hedlin, A review of wind-noise reduction methodologies, in: A. Le Pichon, E. Blanc, A. Hauchecorne (Eds.), *Infrasound Monitoring for Atmospheric Studies*, Springer, Heidelberg. ISBN: 978-1-4020-9507-8, 2010.
[38] C. Ender, *Wind Energy Use in Germany – Status 30 06 2005, DEWI Magazin* 27 (2005) 24–34.
[39] Y. Cansi, An automatic seismic event processing for detection and location: the P.M.C.C. method, *Geophys. Res. Lett.* 22 (1995) 1021–1024, http://dx.doi.org/10.1029/95GL00468.
[40] G.P. Van den Berg, Effects of the wind profile at night on wind turbine sound, *J. Sound Vibr.* 277 (2004) 955–970, http://dx.doi.org/10.1016/j.jsv.2003.09.050.
[41] W.R. Sears, Some aspects of non-stationary air foil theory and its practical application, *J. Aerosp. Sci.* 8 (1941) 104–108, http://dx.doi.org/10.2514/8.10655.
[42] M.V. Lowson, Theoretical analysis of compressor noise, *J. Acoust. Soc. Am.* 47 (1970) 371–385, http://dx.doi.org/10.1121/1.1911508.
[43] M.H. McKenna, R.G. Gibson, B.E. Walker, J. McKenna, N.W. Winslow, A.S. Kofford, Topographic effects on infrasound propagation, *J. Acoust. Soc. Am.* 131 (2012) 35–46, http://dx.doi.org/10.1121/1.3664099.
[44] Steinberg, B., Large aperture teleseismic array theory, Proceedings of the First LASA Systems Evaluation Conference (1965), ARPA-Report, 140p.
[45] K.L. McLaughlin, J.L. Bonner, T. Barker, Seismic source mechanisms for quarry blasts: modelling observed Rayleigh and Love wave radiation patterns from a Texas quarry, *Geophys. J. Int.* 156 (2004) 79–93, http://dx.doi.org/10.1111/j.1365-246X.2004.02105.x.
[46] Gibson, R., D. Norris, InfraMAP: Development of an Infrasound Propagation Modeling Toolkit, DTRA Technical Report (2002). DTRA-TR-99-47.
[47] C. Pilger, F. Streicher, L. Ceranna, K. Koch, Application of propagation modeling to verify and discriminate ground-truth infrasound signals at regional distances, *InfraMatics* 2 (2013) 4, http://dx.doi.org/10.4236/inframatics.2013.24004.
[48] P.T. Negraru, P. Golden, E.T. Herrin, Infrasound propagation in the zone of silence, *Seismol. Res. Lett.* 81 (4) (2010) 614–624, http://dx.doi.org/10.1785/gssrl.81.4.614.
[49] Mutschlecner, J. P., R. W. Whitaker and L. H. Auer, An Empirical Study of Infrasonic Propagation, LA-Report, LA-13620-MS (1999).
[50] L.G. Evers, L. Ceranna, H.W. Haak, A. Le Pichon, R.W. Whitaker, A seismo-acoustic analysis of the gas-pipeline explosion near Ghislenghien in Belgium, *Bull. Seismol. Soc. Am.* 97 (2007) 417–425, http://dx.doi.org/10.1785/0120060061.